Neuron
Article

Synaptic PI(3,4,5)P_3 Is Required for Syntaxin1A Clustering and Neurotransmitter Release

Thang Manh Khuong,[1,2] Ron L.P. Habets,[1,2,5] Sabine Kuenen,[1,2] Agata Witkowska,[4] Jaroslaw Kasprowicz,[1,2] Jef Swerts,[1,2] Reinhard Jahn,[4] Geert van den Bogaart,[3,4] and Patrik Verstreken[1,2,*]
[1]VIB Center for the Biology of Disease, 3000 Leuven, Belgium
[2]KU Leuven, Department of Human Genetics and Leuven Research Institute for Neuroscience and Disease (LIND), 3000 Leuven, Belgium
[3]Department of Tumor Immunology, Radboud University Nijmegen Medical Centre, 6525GA Nijmegen, the Netherlands
[4]Department of Neurobiology, Max-Planck Institute for Biophysical Chemistry, 37077 Göttingen, Germany
[5]Present address: Laboratory of Developmental Neurobiology, Department of Molecular and Cell Biology, Leiden University Medical Center, 2300RC Leiden, the Netherlands.
*Correspondence: patrik.verstreken@cme.vib-kuleuven.be
http://dx.doi.org/10.1016/j.neuron.2013.01.025

SUMMARY

PI(3,4,5)P_3 is a low-abundance lipid thought to play a role in the regulation of synaptic activity; however, the mechanism remains obscure. We have constructed novel split Venus-based probes and used superresolution imaging to localize PI(3,4,5)P_3 at *Drosophila* larval neuromuscular synapses. We find the lipid in membrane domains at neurotransmitter release sites, where it concentrates with Syntaxin1A, a protein essential for vesicle fusion. Reducing PI(3,4,5)P_3 availability disperses Syntaxin1A clusters and increasing PI(3,4,5)P_3 levels rescues this defect. In artificial giant unilamellar vesicles, PI(3,4,5)P_3 also induces Syntaxin1A domain formation and this clustering, in vitro and in vivo, is dependent on positively charged residues in the Syntaxin1A-juxtamembrane domain. Functionally, reduced PI(3,4,5)P_3 causes temperature-sensitive paralysis and reduced neurotransmitter release, a phenotype also seen in animals expressing a Syntaxin1A with a mutated juxtamembrane domain. Thus, our data indicate that PI(3,4,5)P_3, based on electrostatic interactions, clusters Syntaxin1A at release sites to regulate neurotransmitter release.

INTRODUCTION

Phosphoinositides are important cellular signaling lipids, but they are present at very low concentrations in the nervous system (Di Paolo and De Camilli, 2006). While based on their phosphorylation status, seven different phosphoinositides are known at the presynaptic terminal, and phosphatidylinositol 4,5 bisphosphate (PI(4,5)P_2) has been best studied and is involved in a growing number of processes, including the spatial and temporal recruitment of cytosolic proteins that mediate synaptic vesicle cycling and synaptic growth (Cremona et al., 1999; Khuong et al., 2010; Martin, 2012; Verstreken et al., 2009; Wenk et al., 2001). PI(4,5)P_2-dependent recruitment of proteins to specific membrane domains occurs via specific motifs but also by electrostatic interactions with unstructured protein regions that are rich in basic amino acids, inducing the formation of protein-lipid microdomains (Heo et al., 2006; van den Bogaart et al., 2011). In contrast to PI(4,5)P_2, phosphatidylinositol 3,4,5 trisphosphate (PI(3,4,5)P_3) is much less abundant (Clark et al., 2011) and the lipid has been implicated in the clustering of glutamate receptors and postsynaptic density protein-95 in the plasma membrane of postsynaptic terminals (Arendt et al., 2010); however, the mechanism was not elucidated. Contrary to this postsynaptic role, the function of PI(3,4,5)P_3 at presynaptic terminals remains enigmatic.

Here, using transgenic imaging probes based on split Venus, we show that PI(3,4,5)P_3 concentrates in discrete foci and that these foci largely colocalize with presynaptic release sites that are also rich in Syntaxin1A, a SNARE protein essential for synaptic vesicle fusion (Gerber et al., 2008; Schulze et al., 1995). Although phosphorylated phosphoinositides have been implicated in synaptic vesicle endocytosis by interacting with adaptors and other proteins (Cremona et al., 1999; Di Paolo et al., 2004), we find that, unlike reducing PI(4,5)P_2 availability, reducing PI(3,4,5)P_3 levels at presynaptic terminals does not result in significant defects in synaptic vesicle formation. Instead, based on in vitro and in vivo assays, we find that PI(3,4,5)P_3 is critical to induce the clustering of Syntaxin1A and this feature is dependent on the positively charged residues in the Syntaxin1A juxtamembrane domain, suggesting that electrostatic interactions mediate this effect. Either reducing PI(3,4,5)P_3 availability or expressing a Syntaxin1A with a mutated juxtamembrane domain results in reduced neurotransmitter release, similar to partial loss of Syntaxin1A function. Our work thus suggests that presynaptic PI(3,4,5)P_3 is critical to control neurotransmitter release by facilitating Syntaxin1A clustering via electrostatic interactions.

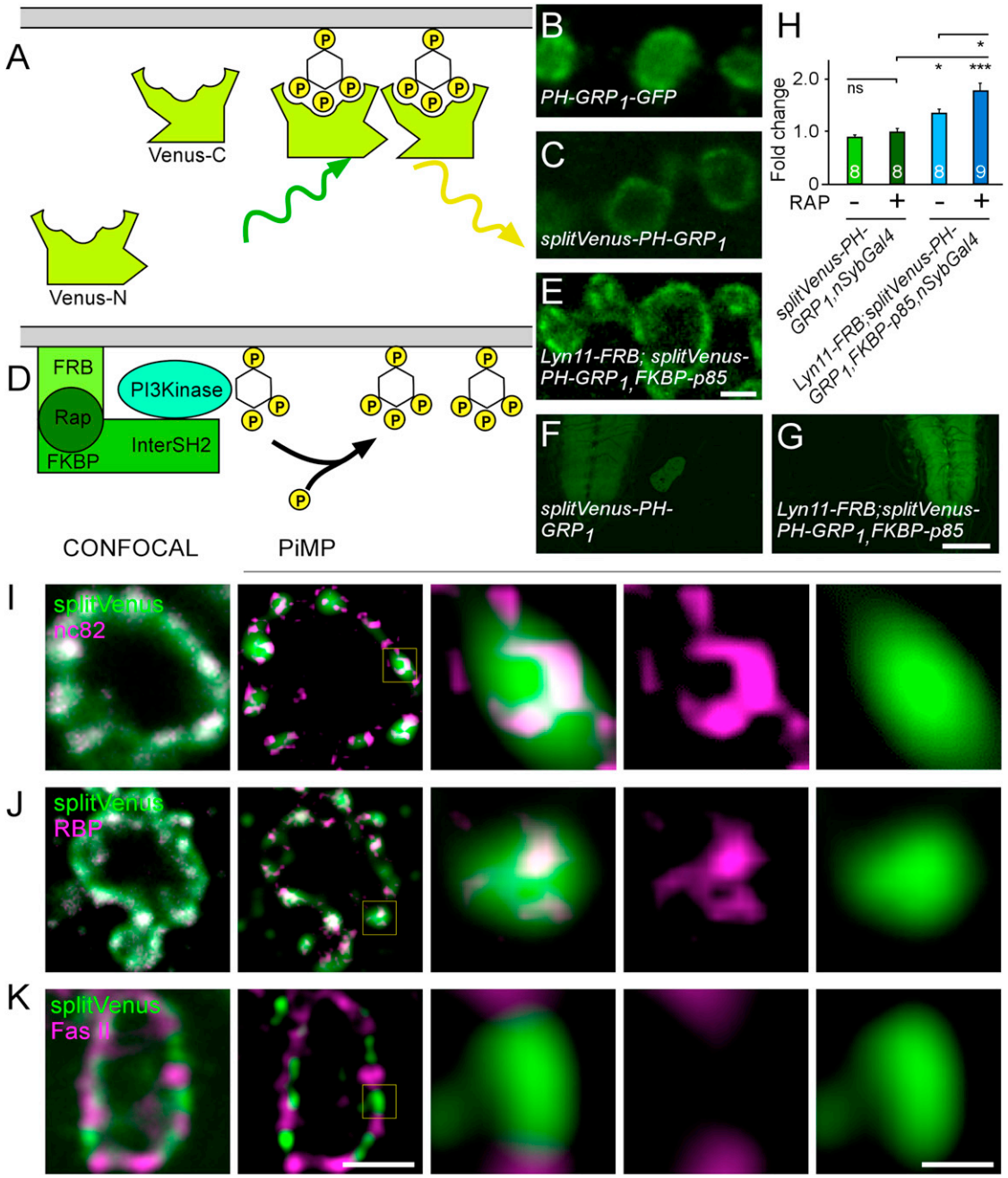

Figure 1. Superresolution Imaging of PI(3,4,5)P_3 Localization at Live Synapses

(A) Schematic of the split Venus-GRP$_1$-PH probe set revealing PI(3,4,5)P_3 localization.

(B) Single confocal section of live imaged third-instar larval *Drosophila* NMJ boutons that express PH-GRP$_1$-GFP (*yw; UAS-PH-GRP$_1$-GFP nSybGal4*).

(C) Single confocal section of live imaged third-instar larval *Drosophila* NMJ boutons that express split Venus-PH-GRP$_1$ (*yw; UAS-VenusC-PH-GRP$_1$, UAS-VenusN-PH-GRP$_1$ nSybGal4*). Note the preferential membrane localization of split Venus-PH-GRP$_1$, in contrast to GFP-PH-GRP$_1$.

(D) Schematic of the tools used to produce PI(3,4,5)P_3 in the presynaptic membrane under control of rapamycin-dependent dimerization of FRB-Lyn11, which is plasma membrane anchored, and FKBP-interSH2, a fusion of FKBP and the SH2 domain of p85 that recruits PI3Kinase, an enzyme that produces PI(3,4,5)P_3.

(E) Single confocal section of live imaged third-instar larval *Drosophila* NMJ boutons of larvae grown on rapamycin expressing FRB-Lyn11, FKBP-p85, and split Venus-PH-GRP$_1$ (*yw; UAS-Lyn11-FRB ; UAS-VenusC-PH-GRP$_1$ UAS-VenusN-PH-GRP$_1$ UAS-FKBP-p85 nSybGal4*). Note the increased Venus signal in the presence of PI3kinase recruitment to the plasma membrane.

(F and G) Live imaging of the ventral nerve cords of larvae grown on rapamycin and expressing split Venus-PH-GRP$_1$ (F) and of larvae grown on rapamycin and expressing FRB-Lyn11, FKBP-p85, and split Venus-PH-GRP$_1$ (*yw; UAS-Lyn11-FRB ; UAS-VenusC-PH-GRP$_1$ UAS-VenusN-PH-GRP$_1$ UAS-FKBP-p85 nSybGal4*) (G). Scale bar in (E) applies to (B), (C), and (E) and represents 2 μm; scale bar in (G) applies to (F) and (G) and represents 100 μm.

(legend continued on next page)

RESULTS

PI(3,4,5)P_3 Localizes to Foci in the Presynaptic Plasma Membrane

PI(3,4,5)P_3 is a low-abundance lipid thought to play a role at the synapse; however, it has not yet been accurately localized in neurons. To assess PI(3,4,5)P_3 localization in vivo at synapses, we created transgenic flies that neuronally (*nSybGal4*) express an EGFP-tagged PH domain of GRP_1 known to preferentially bind PI(3,4,5)P_3 (Britton et al., 2002; Gray et al., 1999; Khuong et al., 2010; Oatey et al., 1999) and monitored EGFP fluorescence at larval neuromuscular junction (NMJ) boutons (Figure 1A). In contrast to several other phosphoinositide binding probes (e.g., 2 × FYVE-GFP or $PLC_{\delta1}$-PH-GFP) (Slabbaert et al., 2012) (see Figure S1A available online), PH-GRP_1-GFP is present throughout the boutons (Figure 1B). PI(3,4,5)P_3 levels are thought to be very low, and we surmise that this "indiscriminate labeling" may be due to a nonbound probe. We therefore developed a split Venus-based probe set (Figure 1A) and coexpressed PH-GRP_1 fused to the N-terminal end of Venus, with PH-GRP_1 fused to the C-terminal end of Venus in neurons using *nSybGal4*. Only when the PH-GRP_1-N- and C-Venus moieties are bound to PI(3,4,5)P_3 they concentrate, and functional Venus fluorescence is visible (Figure 1A). Using this improved strategy, fluorescence associated with the boutonic membrane is clearly visible (Figure 1C and Figure S1A). Furthermore, fluorescence also concentrates at synaptic-rich areas in the neuropile of the ventral nerve cord (Figure 1F), indicating that PI(3,4,5)P_3 is enriched at synapses and is associated with the plasma membrane at synaptic boutons.

To determine whether the split Venus-PH-GRP_1 labeling is specific, we generated transgenic flies that enable PI3kinase to increase the PI(3,4,5)P_3 concentration in the plasma membrane (Figure 1D). We coexpressed the membrane-bound Lyn11-FRB and FKBP-p85 that recruit endogenous PI3kinase in the presence of rapamycin, which is known to mediate the dimerization of FRB and FKBP domains (Spencer et al., 1993; Suh et al., 2006). The concentrations of rapamycin used for dimerization do not noticeably affect neuronal function or development under the conditions that we tested (see below). Thus, growing larvae on rapamycin-containing medium is expected to facilitate recruitment of p85, the PI3Kinase regulatory subunit, to the membrane and to promote the production of PI(3,4,5)P_3. As shown in Figures 1E, 1G, and 1H, growing larvae expressing split Venus-PH-GRP_1, Lyn11-FRB, and FKBP-p85 on rapamycin results in significantly increased boutonic (Figures 1E and 1H, dark blue) and synaptic (Figure 1G) ventral nerve cord fluorescence, compared to equally treated animals that do not express the p85 dimerization tool (Figures 1C, 1F, and 1H, dark green) or compared to larvae expressing split Venus-PH-GRP_1, Lyn11-FRB, and FKBP-p85 larvae that were not placed on rapamycin (Figure 1H, light blue). Note that the split Venus-PH-GRP_1 larvae that express p85 in the absence of rapamycin do show more fluorescence than the controls that do not express p85 (Figure 1H, compare light green to light blue), suggesting that the p85 tool is somewhat leaky. Nonetheless, the fluorescence in split Venus-PH-GRP_1 larvae that express p85 in the absence of rapamycin is still significantly lower than fluorescence measured in the presence of rapamycin (Figure 1H, compare light and dark blue). Thus, the split Venus-PH-GRP_1 probe is a reliable in vivo reporter that recognizes PI(3,4,5)P_3.

Specialized zones for exo- and endocytosis or periactive zones have been defined within the plasma membrane of NMJ boutons. To determine whether PI(3,4,5)P_3 is restricted to specific synaptic membrane domains, we resorted to photobleaching microscopy with nonlinear processing (PiMP) that allows for superresolution imaging beyond the diffraction limit and has been used at *Drosophila* neuromuscular junctions to visualize presynaptic densities (Munck et al., 2012). PiMP imaging of the split Venus-PH-GRP_1 in the presynaptic membrane indicates that the probe concentrates in patches (Figures 1I–1K). These split Venus-PH-GRP_1 patches extensively colocalize with Bruchpilot (anti-BRP^{NC82}) and with RIM binding protein (anti-RBP), which both label aspects of presynaptic release sites (Kittel et al., 2006; Liu et al., 2011) (Figures 1I and 1J). Sixty-eight percent of the presynaptic densities marked by BRP^{NC82} harbor a split Venus-PH-GRP_1 patch. Conversely, split Venus-PH-GRP_1 is largely excluded from regions labeled by anti-FasiclinII that concentrates in periactive zones (Sun et al., 2000) (Figure 1K). Thus, our data indicate that at *Drosophila* third-instar larval boutons, PI(3,4,5)P_3 resident in the plasma membrane concentrates at presynaptic densities where neurotransmitters are released.

PI(3,4,5)P_3 Is Required for Syntaxin1A Clustering at Synaptic Boutons

Expression of the $PLC_{\delta1}$-PH probe shields available PI(4,5)P_2 (Field et al., 2005; Raucher et al., 2000) and reduced levels or availability of PI(4,5)P_2 by expressing $PLC_{\delta1}$-PH or RNAi to PI4P5Kinase both result in reduced levels of boutonic Alpha-adaptin, a PI(4,5)P_2 binding protein (Figures 2A and 2C, green) (González-Gaitán and Jäckle, 1997; Khuong et al., 2010; Verstreken et al., 2009; Zoncu et al., 2007). Similarly, to determine whether synaptic PI(3,4,5)P_3 is required for the localization of Alpha-adaptin, we expressed the PH-GRP_1 to shield PI(3,4,5)P_3 and we used RNAi to PI3Kinase92E, a PI(3,4,5)P_3-producing enzyme. However, the abundance of Alpha-adaptin is not altered when expressing PH-GRP_1 or when knocking down PI3Kinase92E (Figures 2A and 2B, green, and Figure S2A). These data suggest that synaptic PI(4,5)P_2 availability is not majorly affected when lowering PI(3,4,5)P_3 levels and that boutonic Alpha-adaptin localization is less sensitive to alterations in PI(3,4,5)P_3 availability.

(H) Quantification of split Venus-PH-GRP_1 fluorescence at synaptic boutons in the genotypes indicated in (C) and (E) in the presence and absence of rapamycin. Data are represented as mean ± SEM; n is indicated in the bars; ANOVA, Tukey's test: *$p < 0.05$, ***$p < 0.001$; ns, not significant.

(I–K) Superresolution PiMP imaging (right) of single confocal sections (left) of split Venus-GRP_1-PH-expressing animals on rapamycin (*yw; UAS-Lyn11-FRB ; UAS-VenusC-PH-GRP_1 UAS-VenusN-PH-GRP_1 UAS-FKBP-p85 nSybGal4*) through the center of synaptic boutons labeled with BRP^{NC82} (NC82) (I), RIM binding protein (RBP) (J), or FasicilinII (FasII) (K). Related to Figure S1. Scale bars in (K) apply to (I)–(K) and represent 2 μm on the left and 200 nm on the right.

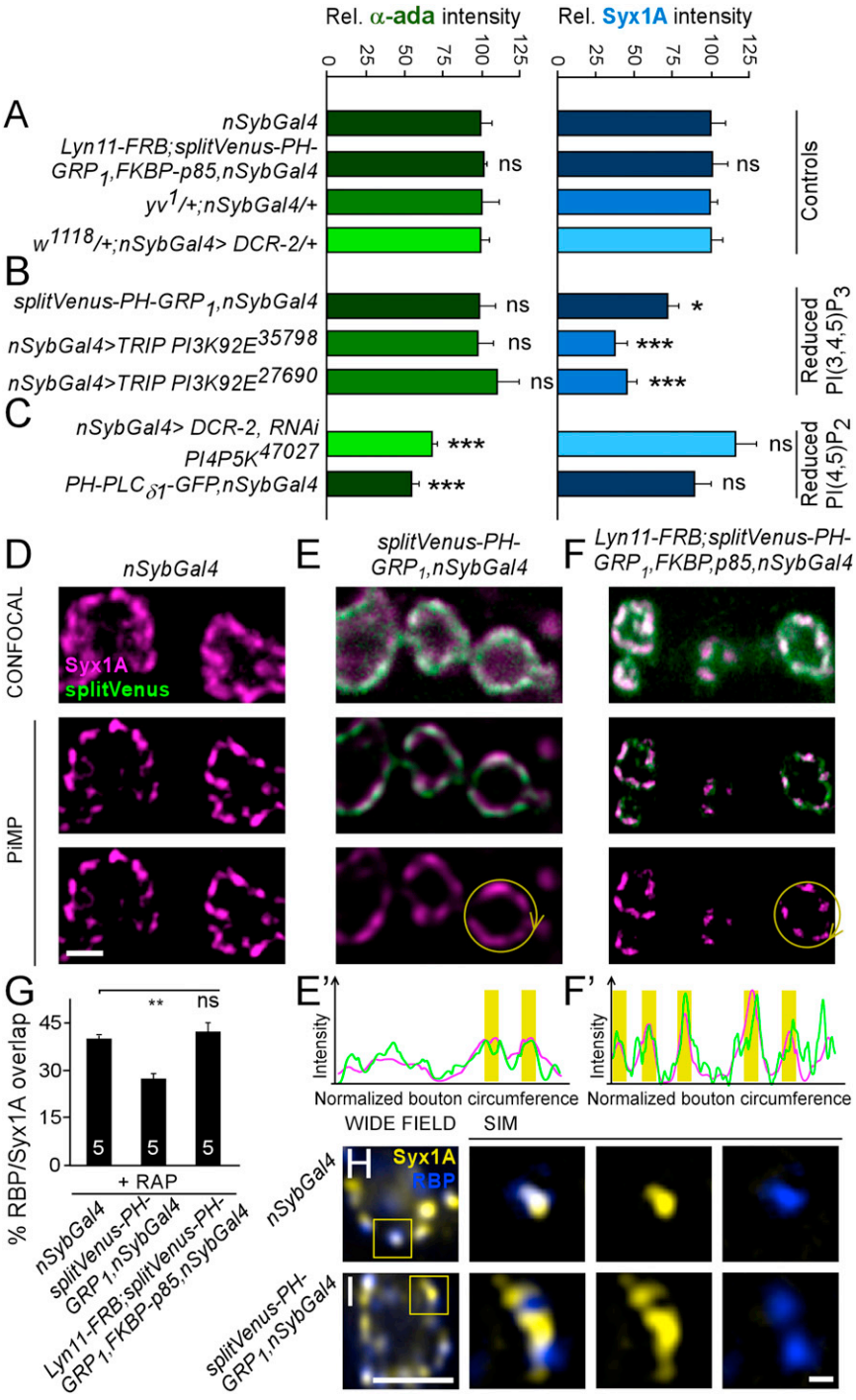

Figure 2. Reduced PI(3,4,5)P_3 Availability Results in Reduced Synaptic Syntaxin1A Clustering at Active Zones

(A–C) Alpha-Adaptin (green) and Syntaxin1A (blue) labeling intensities at third-instar boutons of controls (A; *yw; nSybGal4* and *yw; UAS-Lyn11-FRB ; UAS-VenusC-PH-GRP$_1$ UAS-VenusN-PH-GRP$_1$ UAS-FKBP-p85 nSybGal4* and *yv^1/+; nSybGal4/+* and *w UAS-DCR-2/w^{1118}; nSyb-Gal4/+*), of animals with reduced levels or availability of PI(3,4,5)P_3 (B; *yw; UAS-VenusC-PH-GRP$_1$ UAS-VenusN-PH-GRP$_1$ nSybGal4* and *UAS-TRIP(PI3K92E$^{35798\ or\ 27690}$/nSybGal4*), and of animals with reduced levels or availability of PI(4,5)P_2 (C; *w UAS-DCR-2/w^{1118};UAS-PI4P5K^{47027}/nSybGal4* and *UAS-PH-PLC$_{\delta1}$-GFP nSybGal4*). Related to Figure S2. Data are represented as mean ± SEM; ANOVA, Tukey's test: *p < 0.05, ***p < 0.001; ns, not significant (in comparison to control bars of the same shade).

(D–F) Single confocal section of third-instar larval *Drosophila* NMJ boutons labeled with anti-syntaxin1A^{8C3} (Syx1A, magenta) of controls (D), of split Venus-PH-GRP$_1$-expressing (green) animals (E), and of FRB-Lyn11-, FKBP-p85-, and split Venus-PH-GRP$_1$-expressing animals (F) all grown on rapamycin (top) and the same area imaged using superresolution PiMP (bottom). (E′ and F′) Fluorescence intensity plots (arbitrary units) along the circumference of the bouton indicated in (E) or (F), starting at the arrow point, in the direction of the arrow, adjusted to the total bouton circumference of anti-Syntaxin1A labeling intensity and of split Venus fluorescence intensity. Yellow highlighted sections mark peaks of labeling. Related to Figure S2. Scale bar in (D) applies to (D)–(F) and represents 2 μm.

(G–I) Quantification (G) of the overlap between Syntaxin1A labeling and RBP labeling (yellow) and RBP labeling (blue; H and I) in SR-SIM images (left in H and I) of control (H), split Venus-PH-GRP$_1$-expressing animals (I), and of FRB-Lyn11-, FKBP-p85-, and split Venus-PH-GRP$_1$-expressing animals all on rapamycin and wide-field and superresolution SR-SIM imaging of the same areas (H and I, right). Scale bars in (I) represent 2 μm on the left and 200 nm on the right. Data are represented as mean ± SEM; n is indicated in the bars; ANOVA, Dunnett's test: *p < 0.05.

Next, we tested whether expression of PH-GRP$_1$ affects the localization or abundance of other synaptic proteins, including Dap160, EndoA, and CSP, as well as the active zone marker BRP (Kittel et al., 2006; Koh et al., 2004; Marie et al., 2004; Verstreken et al., 2002; Wagh et al., 2006; Zinsmaier et al., 1994), but we find that these are not affected upon expression of PH-GRP$_1$ (Figures S2A–S2E). Finally, we assessed the abundance of Syntaxin1A, a protein essential for synaptic vesicle fusion (Schulze et al., 1995) that enriches to PI(4,5)P_2-containing microdomains in PC12 cells (Aoyagi et al., 2005; van den Bogaart et al., 2011). Expression of PH-GRP$_1$ results in significantly less Syntaxin1A labeling at synaptic boutons (Figures 2A and 2B, blue). This effect is caused by reduced PI(3,4,5)P_3 availability, as RNAi to PI3Kinase92E also results in less Syntaxin1A labeling and coexpression of the PH-GRP$_1$ probe together with the Lyn11-FRB/FKBP-p85 in the presence of rapamycin restores the Syntaxin1A labeling defect (Figures 2A and 2B, blue). In contrast, expression of the PLC$_{\delta1}$-PH probe that shields

PI(4,5)P_2 or RNAi to PI4P5Kinase does not significantly affect Syntaxin1A labeling intensity at neuromuscular boutons (Figures 2A and 2C). The data suggest that Syntaxin1A levels in *Drosophila* third-instar bouton membranes are more sensitive to PI(3,4,5)P_3 availability than they are to PI(4,5)P_2.

PI(3,4,5)P_3 localizes to presynaptic microdomains in the membrane, and to investigate whether Syntaxin1A also concentrates at these sites, we used superresolution PiMP and SR-SIM imaging. We find that in control boutons, Syntaxin1A is enriched in plasma membrane-bound domains (Figure 2D), and these domains extensively colocalize with the active zone marker RBP (Figures 2G and 2H). Interestingly, in boutons that express PH-GRP$_1$, these Syntaxin1A domains are largely dispersed (Figures 2E and 2E′) and much less Syntaxin1A colocalizes with RBP (Figures 2G and 2I). Indicating that this defect is specific to reduced PI(3,4,5)P_3 levels, Syntaxin1A in PH-GRP$_1$, Lyn11-FRB/FKBP-p85-expressing animals placed on rapamycin now again concentrates in defined clusters that colocalize with split Venus-PH-GRP$_1$ (Figures 2F and 2F′; 73% of the GRP$_1$ puncta overlap with a Syntaxin1A spot) and with anti-RBP (Figure 2G). Thus, at *Drosophila* neuromuscular boutons, Syntaxin1A largely colocalizes with PI(3,4,5)P_3 at active zones, and this Syntaxin1A localization is dependent on the presence of PI(3,4,5)P_3. Finally, also in PC12 cell membrane sheets that we labeled using recombinant GRP$_1$-PH-mCherry and anti-Syntaxin1A antibodies, we find extensive colocalization (Figure S2F; 84% of the GRP1 puncta overlap with a Syntaxin1A spot), and this colocalization is more prevalent than when membrane sheets were labeled with PLC$_{\delta1}$-PH-GFP and anti-Syntaxin1A (van den Bogaart et al., 2011). Hence, access to PI(3,4,5)P_3 is necessary for the formation of normal Syntaxin1A domains in the membrane in vivo.

PI(3,4,5)P_3 Is Sufficient for Syntaxin1A Clustering In Vitro

To test whether PI(3,4,5)P_3 harbors the intrinsic property to mediate Syntaxin1A clustering in membranes, we turned to a heterologous system and prepared DiO-labeled giant unilamellar vesicles (GUVs) (8:2 molar ratio of DOPC and DOPS [1,2-dioleoyl-sn-glycero-3-phosphatidylcholine and -serine]) in which we incorporated 3 mol% of an Atto647N-labeled Syntaxin1A peptide comprising the polybasic linker and the transmembrane helix, allowing us to detect Syntaxin1A distribution in the GUV membrane. While GUVs without PI(3,4,5)P_3 show uniform membrane labeling of Syntaxin1A (Figure 3A), adding 1.5 mol% PI(3,4,5)P_3 in the GUV membrane results in profound clustering of the Syntaxin1A protein (Figure 3B). Thus, in line with our in vivo studies at NMJ boutons, PI(3,4,5)P_3 facilitates lateral Syntaxin1A clustering in membranes.

Syntaxin1A is an integral membrane protein that harbors several charged lysine and arginine residues in its juxtamembrane domain and these residues are in close contact with the lipid head groups of the inner lipid leaflet (James et al., 2008; Kweon et al., 2002; van den Bogaart et al., 2011). This stretch of positively charged residues is conserved across species (Table S1), suggesting that it is functionally important; previous data indicate that these Syntaxin1A residues electrostatically interact with PI(4,5)P_2 (Kweon et al., 2002; van den Bogaart et al., 2011). PI(4,5)P_2 harbors a net charge of −3.99 ± 0.10, while the net charge of PI(3,4,5)P_3 is even more negative: −5.05 ± 0.15 at physiological pH 7.0 (Kooijman et al., 2009). We therefore wondered whether the basic juxtamembrane residues would be involved in mediating PI(3,4,5)P_3-dependent Syntaxin1A clustering. To test this hypothesis, we incorporated an Atto647N-labeled "KARRAA" mutant Syntaxin1A peptide, in which two of the lysines are mutated to a neutral alanine, in the GUVs and tested clustering of the protein in the presence of PI(3,4,5)P_3. Mutating these two amino acids abolishes the ability of PI(3,4,5)P_3 to cluster Syntaxin1A in GUV membranes (Figure 3C), suggesting that PI(3,4,5)P_3-mediated Syntaxin1A clustering is facilitated by electrostatic interactions and that these interactions are sufficient for PI(3,4,5)P_3-Syntaxin1A domain formation.

Next, to compare the strength of the interaction between Syntaxin1A and PI(3,4,5)P_3 to the interaction between Syntaxin1A and PI(4,5)P_2, we used a fluorescence resonance energy transfer (FRET)-based competition assay (Murray and Tamm, 2009). We prepared 100-nm-sized liposomes loaded with the Atto647N-labeled Syntaxin1A peptide (residues 257–288) and Bodipy-TMR PI(4,5)P_2, in which Atto647N, the acceptor fluorphore and Bodipy-TMR, the donor fluorphore, are a FRET pair (van den Bogaart et al., 2011) (Figure 3D). Adding a 1:1 or a 1:10 ratio of unlabeled to labeled PI(4,5)P_2 results in a 16% and 44% reduction in FRET efficiency, respectively (Figures 3E and 3F). Interestingly, adding only a 1:1 ratio of unlabeled PI(3,4,5)P_3 to labeled PI(4,5)P_2 already results in a 45% reduction in FRET efficiency (Figures 3E and 3F). Hence, the data indicate that PI(3,4,5)P_3 interacts more efficiently with Syntaxin1A than does PI(4,5)P_2, in line with the in vivo data at NMJ boutons that indicate that reduced PI(3,4,5)P_3 levels result in reduced Syntaxin1A clustering (Figure 2).

To test whether the positive charges in the Syntaxin1A juxtamembrane domain are also needed for clustering of the protein at synapses in vivo, we used recombination in yeast to generate hemagglutinin (HA)-tagged fruit fly Syntaxin1A^{KARRAA} or HA-tagged wild-type Syntaxin1A. The genomic constructs were inserted using Phi-C-31 integrase at the identical genomic location (25C6) and the proteins are expressed under endogenous fruit fly promotor control. We then assessed the localization of these proteins in relation to the active zone marker RBP. Compared to wild-type HA-Syntaxin1A, the mutant HA-Syntaxin1A^{KARRAA} overlaps much less with the active zone marker RBP and the mutant protein appears more dispersed (Figures 3G–3I). The data are consistent with a model in which Syntaxin1A concentrates with PI(3,4,5)P_3 in membranes based on electrostatic interactions between negatively charged PI(3,4,5)P_3 head groups and positively charged juxtamembrane residues, resulting in the formation of circular domains in which boundary energy is minimized (Christian et al., 2009). While such a mechanism has previously been proposed for PI(4,5)P_2-Syntaxin1A-mediated interactions (Aoyagi et al., 2005; Lam et al., 2008; McLaughlin and Murray, 2005; van den Bogaart et al., 2011), taken together, our in vivo and in vitro data suggest a critically important role for the more negatively charged PI(3,4,5)P_3 in Syntaxin1A clustering at synapses.

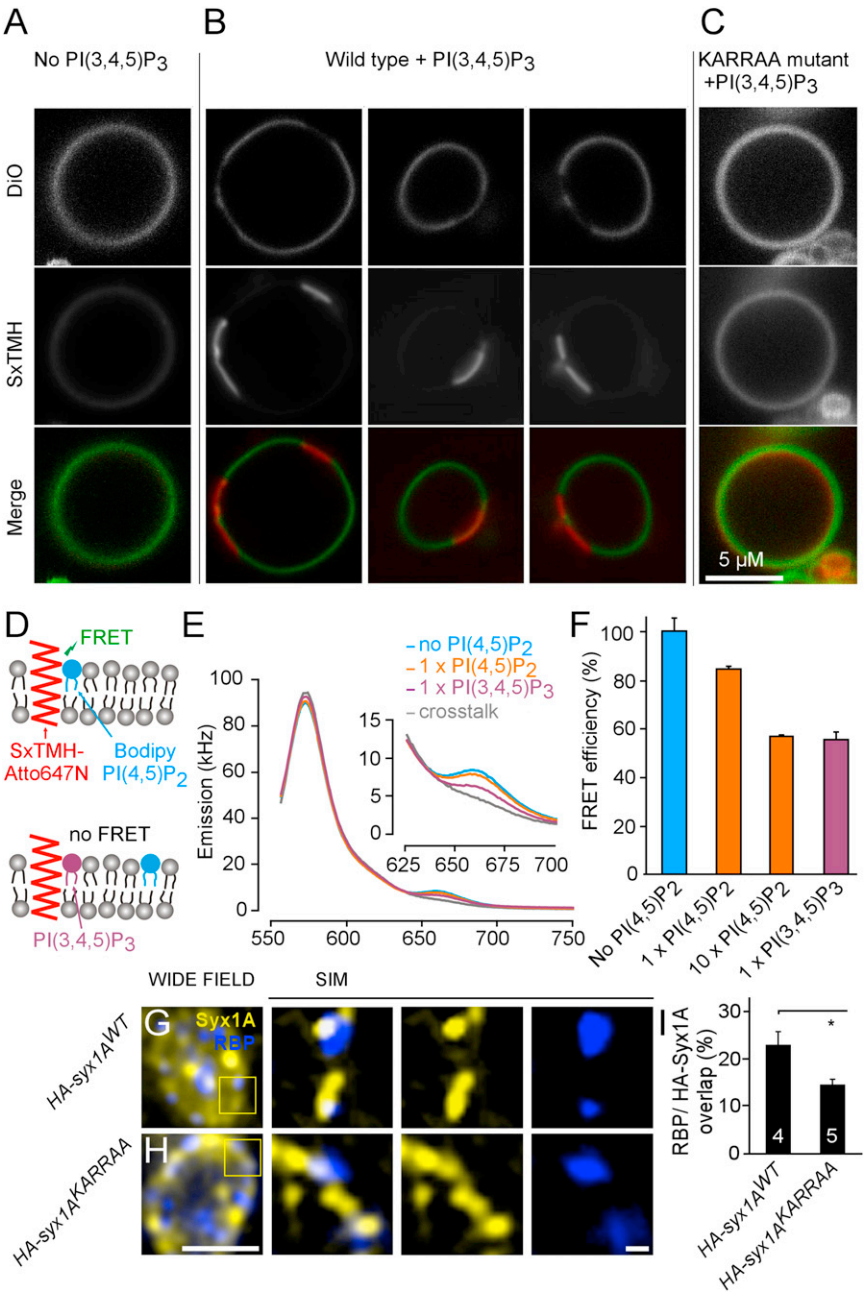

Figure 3. Syntaxin1A Clusters with PI(3,4,5)P_3 Based on Electrostatic Interactions

(A–C) Confocal imaging of the synthetic C-terminal peptide of Syntaxin1A (residues 257–288) labeled with Atto647N (red) reconstituted in GUVs at a 1:30 molar protein to lipid ratio. The lipid mix is DOPC with 20% DOPS, 1.5% DiO (3,3′-dioctadecyloxacarbocyanine; green), and without (A) or with (B) 1.5 mol% PI(3,4,5)P_3. (C) Confocal imaging of the synthetic C-terminal peptide of Syntaxin1A from which two positively charged residues were changed from the polybasic linker (K264A K265A; 260-KARRAA) reconstituted in GUVs at a 1:30 molar protein to lipid ratio (see A and B) with 1.5 mol% PI(3,4,5)P_3. Related to Table S1.

(D–F) FRET-based competition binding experiment (Murray and Tamm, 2009): the interaction between bodipy-PI(4,5)P_2 (cyan; donor fluorophore) and Atto647N-labeled Syntaxin1A (257–288) (red; acceptor fluorophore) results in FRET (van den Bogaart et al., 2011). Unlabeled PI(3,4,5)P_3 (purple) competes with the bodipy-PI(4,5)P_2 Syntaxin1A binding reducing FRET (D). Emission spectra (E) of 100-nm-sized liposomes with a 1:5,000 molar protein-to-lipid ratio of Atto647N-labeled Syntaxin1A (257–288) and 1:5,000 of bodipy-PI(4,5)P_2. Inclusion of 1:5,000 of unlabeled PI(4,5)P_2 (1 × PI(4,5)P_2; orange), 1:500 of unlabeled PI(4,5)P_2 (10 × PI(4,5)P_2; orange in F), or 1:5,000 of unlabeled PI(3,4,5)P_3 (1 × PI(3,4,5)P_3; purple) results in a reduction of FRET and a spectrum in the presence of 0.05% Triton X-100 was recorded to correct for the fluorescence crosstalk (gray). (F) Quantification of the competitive binding of data in (E). Shown is the ratio of acceptor (at 661 nm) over the donor emission (at 572 nm) after correction of crosstalk (emission at 661 nm in the presence of Triton X-100). Error bars represent SD of two independent experiments, each repeated three times.

(G–I) Wide-field (G and H, left) and SR-SIM images (magnification in G and H, right) of Syntaxin1A-labeled (anti-HA, yellow) and RBP-labeled (blue) boutons of control (*yw; HA-syx1A^{WT}*; G) and of animals expressing a Syntaxin1A with a mutant juxtamembrane domain (*yw; HA-syx1A^{KARRAA}*; H) and quantification of the overlap between Syntaxin1A and RBP (I). Scale bars in (H) represent 2 µm on the left and 200 nm on the right. Data are represented as mean ± SEM; n is indicated in the bars; ANOVA, Tukey's test: *p < 0.05.

Reduced PI(3,4,5)P_3 Availability Results in Synaptic Transmission Defects

Numerous mutations that affect synaptic transmission result in adult temperature-sensitive paralysis in fruit flies, including *dap160*, *shibire (dynamin)*, *syntaxin1A*, *CSP*, and *comatose (NSF)* (Koh et al., 2004; Littleton et al., 1998; Zinsmaier et al., 1994). To test whether reduced PI(3,4,5)P_3 availability in the nervous system results in temperature-dependent paralysis, we placed flies that express PH-GRP$_1$ under control of the neuronal *nSybGal4* driver in an empty vial in a water bath at different temperatures and counted the number of flies standing after 3 min. In contrast to controls, PH-GRP$_1$-expressing flies show a dose-dependent temperature sensitivity and at 38°C all flies are paralyzed within 3 min (Figures 4A and 4B). When flies are placed back at room temperature, they recover slowly (data not shown). This effect is specific to reduced availability of PI(3,4,5)P_3, as expressing the PH-GRP$_1$ probe together with the Lyn11-FRB/FKBP-p85 and growing the animals on rapamycin completely rescues temperature-sensitive paralysis and animals behave like controls in this assay (Figure 4C). Indicating dose dependency, Lyn11-FRB/FKBP-p85 in the absence of rapamycin, a condition that results in a marginal

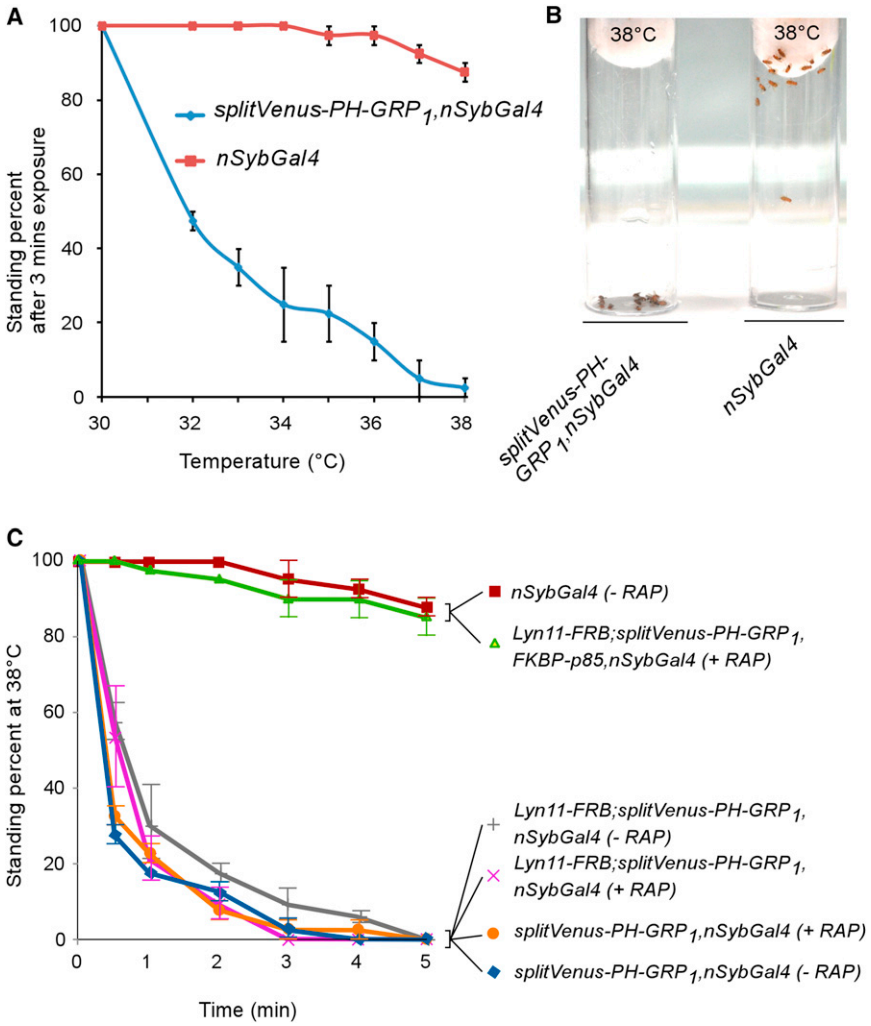

Figure 4. PI(3,4,5)P_3 Is Required for Normal Coordination at Elevated Temperatures

(A and B) Temperature-sensitive behavior of flies expressing split Venus-PH-GRP$_1$ (*yw; UAS-VenusC-PH-GRP$_1$ UAS-VenusN-PH-GRP$_1$ nSybGal4*) and of control flies (*nSybGal4*) measured as percentage of flies standing after 3 min of exposure to the indicated temperatures (A) and foto of split Venus PH-GRP$_1$ expressing flies and controls for 3 min at 38°C (B).

(C) Percent flies standing at 38°C for the indicated period of time of the genotypes indicated. "−RAP' indicates flies were not fed rapamycin and "+ RAP" indicates flies were fed rapamycin. Note that temperature-sensitive paralysis of flies expressing split Venus-PH-GRP$_1$ is rescued by coexpression of Lyn11-FRB and FKB-p85 on rapamycin. Data are represented as mean ± SEM; n = 20 per genotype.

increase in PI(3,4,5)P_3 (Figure 1H), results in a very partial, incomplete rescue of the temperature-sensitive paralysis induced by expression of PH-GRP$_1$ (Figure 4C). Thus, reduced PI(3,4,5)P_3 levels result in temperature-sensitive paralysis in line with defects in neuronal function.

To test whether reduced PI(3,4,5)P_3 availability in neurons affects presynaptic function, we expressed PH-GRP$_1$ using *nSybGal4* and tested synaptic vesicle cycling efficiency using FM1-43 after a 1 min 90 mM KCl stimulation period (Ramaswami et al., 1994). FM1-43 binds membranes, becomes fluorescent, and is internalized into synaptic vesicles upon nerve stimulation. We quantified fluorescence of internalized FM1-43 at NMJ boutons and find a significant reduction of FM1-43 labeling in the PH-GRP$_1$-expressing animals compared to controls (*nSybGal4*) (Figures 5A and 5E). Again, coexpression of Lyn11-FRB/FKBP-p85 in the presence of rapamycin rescues the defect in FM1-43 dye uptake to a level similar to controls (*nSybGal4* with rapamycin) (Figures 5B–5E). These data indicate that reduced PI(3,4,5)P_3 availability dampens synaptic vesicle cycling.

Reduced stimulus-dependent FM1-43 dye uptake may be the result of impaired synaptic vesicle endocytosis or because of a defect in synaptic vesicle fusion. Defects in synaptic endocytosis are often detectable using transmission electron microscopy, revealing stalled endocytic intermediates, an increased number of cisternae, and reduced synaptic vesicle density (Kasprowicz et al., 2008; Verstreken et al., 2009). We assessed the ultrastructure of synaptic boutons of controls and PH-GRP$_1$-expressing animals, but we did not observe endocytic intermediates or cisternae, nor did we measure a reduction in synaptic vesicle density (Figure S3). Thus, these data indicate that expression of PH-GRP$_1$ under these conditions does not majorly affect synaptic vesicle endocytosis, in contrast to expression of PLC$_{\delta1}$-PH that shields PI(4,5)P_2 and results in reduced synaptic vesicle endocytosis, as well as in the mislocalization of endocytic proteins that are known to bind PI(4,5)P_2 (e.g., Alpha-adaptin) (Cremona et al., 1999; Khuong et al., 2010; Verstreken et al., 2009).

To test whether expression of PH-GRP$_1$ affects vesicle fusion and neurotransmitter release, we performed two-electrode voltage-clamp (TEVC) experiments and recorded excitatory junctional currents (EJCs) at the third-instar larval NMJ. Compared to controls, EJC amplitudes recorded from PH-GRP$_1$-expressing animals are significantly reduced (Figures 5F and 5G). Consistent with the defect caused by reduced PI(3,4,5)P_3 availability, neuronally expressed RNAi to PI3Kinase92E also results in a lower EJC amplitude, and expression of Lyn11-FRB/FKBP-p85 in the presence of rapamycin can rescue the lower EJC amplitudes measured in animals that express PH-GRP$_1$ to the level measured in controls (*nSybGal4* with and without rapamycin). Thus, neuronal PI(3,4,5)P_3 is required for normal synaptic transmission.

Syntaxin1A is required for neurotransmitter release (Schulze et al., 1995) and the lower EJC amplitudes we measured upon

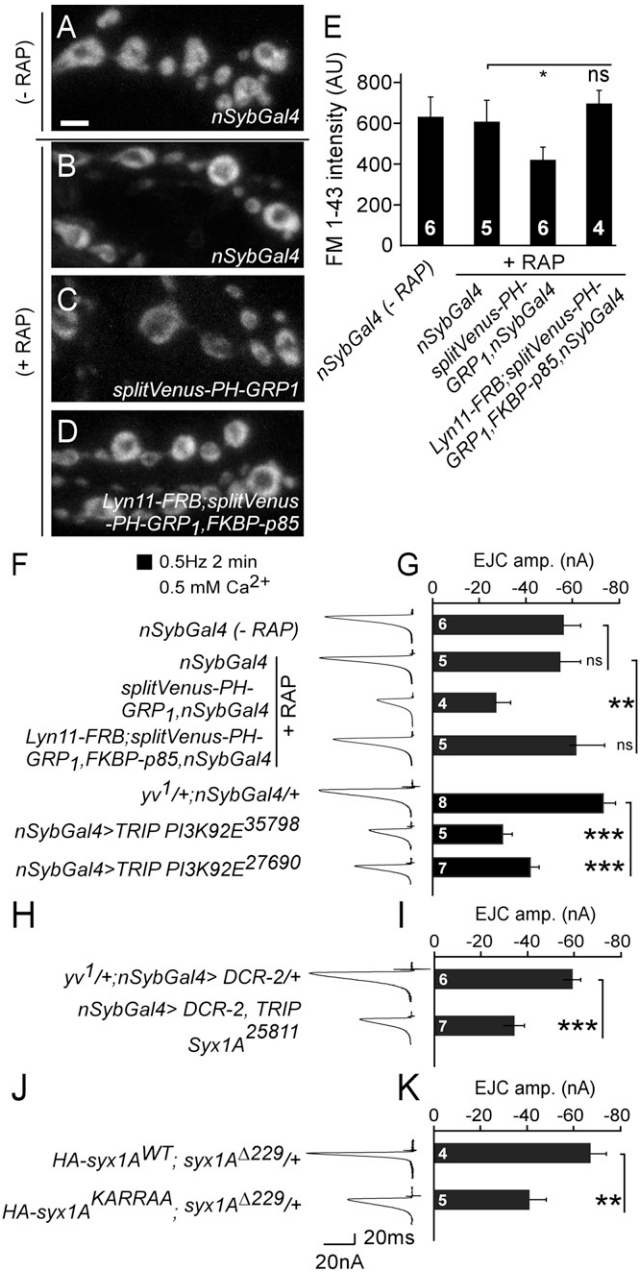

Figure 5. PI(3,4,5)P_3 Is Required for Neurotransmitter Release

(A–E) Imaging of FM1-43 dye internalized into synaptic boutons at the third-instar larval NMJ during a 1 min 90 mM KCl stimulation protocol in control with and without rapamycin (*nSybGal4* "– RAP" and "+ RAP"; A and B), in animals neuronally expressing split Venus-PH-GRP_1 (*yw; UAS-VenusC-PH-GRP_1 UAS-VenusN-PH-GRP_1 nSybGal4*; C) and in animals expressing Lyn11-FRB, FKBP-p85, and split Venus-PH-GRP_1 (*yw; UAS-Lyn11-FRB ; UAS-VenusC-PH-GRP_1 UAS-VenusN-PH-GRP_1 UAS-FKBP-p85 nSybGal4*; D), both with rapamycin as well as quantification of boutonic FM1-43 fluorescence (E). Related to Figure S3.

(F and G) Excitatory junctional current traces (F) and quantification of their average amplitude (G) of recordings made in 0.5 mM calcium in control (*nSybGal4*) with and without rapamycin, in animals neuronally expressing split Venus-PH-GRP_1, in animals expressing FRB-Lyn11, FKBP-p85, and split Venus-PH-GRP_1 with rapamycin, and in animals neuronally expressing *UAS-TRIP(PI3K92E$^{35798\ or\ 27690}$)* to reduce PI(3,4,5)P_3 levels, as well as their controls (*yv^1/+; nSybGal4/+*).

(H and I) Excitatory junctional current traces (H) and quantification of their average amplitude (I) of recordings made in 0.5 mM calcium in control (*w UAS-DCR-2/yv^1; nSybGal4/+*) and in animals neuronally expressing *UAS-TRIP(Syx1A^{25811})*.

(J and K) Excitatory junctional current traces (J) and quantification of their average amplitude (K) of recordings made in 0.5 mM calcium in heterozygous *syntaxin1A* mutant animals expressing wild-type Syntaxin1A (*HA-syx1A^{WT}; syx1A$^{\Delta 229}$/+*) and in heterozygous *syntaxin1A* mutant animals expressing mutant Syntaxin1A^{KARRAA} (*HA-syx1A^{KARRAA}; syx1A$^{\Delta 229}$/+*). Data are represented as mean ± SEM; n is indicated in the bars; for (G), ANOVA, Tukey's test; for (I) and (K), t test: **p < 0.01; ***p < 0.001; ns, not significant.

reducing PI(3,4,5)P_3 levels or availability are consistent with reduced Syntaxin1A-clustering and function. Indeed, RNAi to Syntaxin1A (69.6% ± 4.3% knockdown by boutonic immunolabeling) results in an ~50% reduction in EJC amplitude (Figures 5H and 5I). To further test whether Syntaxin1A binding to PI(3,4,5)P_3 is critical for neurotransmitter release, we also measured EJCs in animals that express HA-Syntaxin1A^{KARRAA}. Given that *syntaxin1A$^{\Delta 229}$* null mutants (Schulze et al., 1995) expressing mutant HA-Syntaxin1A^{KARRAA} are embryonic lethal, we tested for a dominant effect on neurotransmission and measured EJCs in heterozygous *syntaxin1A$^{\Delta 229}$* larvae that are homozygous for the HA-Syntaxin1A^{KARRAA} or the wild-type HA-Syntaxin1A transgene. Compared to animals that express wild-type HA-Syntaxin1A, EJC amplitudes in HA-Syntaxin1A^{KARRAA}-expressing animals are significantly reduced (Figures 5J and 5K), indicating that HA-Syntaxin1A^{KARRAA} interferes with Syntaxin1A function. Taken together, the data are consistent with a model in which PI(3,4,5)P_3 regulates Syntaxin1A clustering at active zones, thus controlling synaptic vesicle fusion efficiency.

DISCUSSION

In this work, we have uncovered a role for PI(3,4,5)P_3 in synaptic transmission. Although PI(3,4,5)P_3 is present at low levels, using split Venus probes that preferentially recognize PI(3,4,5)P_3, together with superresolution imaging, we find that in the presynaptic membrane of *Drosophila* neuromuscular boutons, PI(3,4,5)P_3 concentrates in foci. We show that these PI(3,4,5)P_3 domains colocalize with presynaptic release sites rich in Syntaxin1A in vivo, as well as with Syntaxin1A foci in PC12 cells. PI(3,4,5)P_3 is known to cluster in other cell types as well, and the lipid regulates various cellular processes, including ion channel function (Di Paolo and De Camilli, 2006); however, in our manipulations, we did not observe major effects on action potential initiation or propagation when electrically stimulating motor neurons. At synapses, the localization of PI(3,4,5)P_3 at neurotransmitter release sites is consistent with a role in neurotransmitter release and our electrophysiological analyses are in support of this notion.

We find that reduced levels or availability of PI(3,4,5)P_3 in live neurons results in adult temperature-sensitive paralysis and reduced neurotransmitter release, but not in reduced synaptic vesicle endocytosis under the conditions tested. In contrast, neuronal expression of $PLC_{\delta 1}$-PH that reduces PI(4,5)P_2

availability results in the mislocalization of endocytic proteins that bind PI(4,5)P_2, as well as in reduced synaptic vesicle formation, but it does not affect exocytosis of neurotransmitters under the conditions we tested (Khuong et al., 2010; Verstreken et al., 2009). Furthermore, reducing PI(4,5)P_2 but not PI(3,4,5)P_3 levels in *Drosophila* motor neurons results in neuromuscular junction growth defects (Khuong et al., 2010). Previous work has implicated PI(4,5)P_2 in vesicle fusion in neuroendocrine cells and other cell types (Di Paolo et al., 2004; Martin, 2012; Milosevic et al., 2005), and we cannot exclude that upon expression of $PLC_{\delta1}$-PH, sufficient "free" PI(4,5)P_2 remains to mediate vesicle fusion at synapses. Nonetheless, our data indicate that very distinct processes are more sensitive to reduced levels of either of these phosphoinositides such that reduced PI(3,4,5)P_3 levels preferentially impinge on the exocytic process, while reduced PI(4,5)P_2 affects vesicle formation by mediating the recruitment of endocytic protein complexes (Di Paolo and De Camilli, 2006; Zoncu et al., 2007).

The biophysical properties of PI(4,5)P_2 enable coclustering of proteins with stretches of basic amino acids based on electrostatic interactions (Denisov et al., 1998; McLaughlin and Murray, 2005). PI(4,5)P_2 holds a net negative charge of about −4 and has been suggested to act as a charge bridge spanning the distance between different Syntaxin1A moieties (van den Bogaart et al., 2011). Our data now suggest that the more negatively charged PI(3,4,5)P_3 (net charge of about −5) plays a critical role in Syntaxin1A clustering in vivo. First, shielding PI(3,4,5)P_3 disperses Syntaxin1A clusters at *Drosophila* larval neuromuscular junctions and this defect is rescued by increasing synaptic PI(3,4,5)P_3 levels. Second, reducing PI(3,4,5)P_3 levels in neurons results in reduced synaptic transmission similar to partial loss of Syntaxin1A, and, third, PI(3,4,5)P_3 in GUVs and at NMJ synapses creates Syntaxin1A domains, and these are dependent on the positively charged juxtamembrane residues in Syntaxin1A. Hence, our work defines a critical role for presynaptic PI(3,4,5)P_3 in the clustering of Syntaxin1A at neurotransmitter release sites.

Functionally, we find that Syntaxin1A is an important mediator of the reduced synaptic transmission seen at synapses with reduced PI(3,4,5)P_3 levels. Indeed, reducing PI(3,4,5)P_3 levels or expressing the PI(3,4,5)P_3 binding-defective Syntaxin1A^{KARRAA} results in reduced neurotransmitter release. Hence, at the level of neurotransmission, our data suggest that PI(3,4,5)P_3 acts via Syntaxin1A, but other proteins that can electrostatically interact with phosphoinositides may harbor additional regulatory roles as well (Hammond et al., 2012).

Unlike the recruitment of phosphoinositide binding proteins from the three-dimensional cytoplasmic space, Syntaxin1A coclustering with PI(3,4,5)P_3 occurs by slowed lateral diffusion in the two-dimensional presynaptic plasma membrane. We reason that specific lipid subtypes are ideally positioned to create microdomains with membrane-associated proteins such as Syntaxin1A but probably also with other membrane-bound proteins with basic residues that harbor phosphoinositide affinity (Wang et al., 2002). In this model, membrane phosphoinositide lipid composition would define local protein clustering at the plasma membrane but possibly also at other intracellular organelle membranes that are each characterized by different phosphoinositides (Di Paolo et al., 2004; Hammond et al., 2012). Furthermore, it is tempting to speculate that different Syntaxin isoforms present on these intracellular organelle membranes are also cluster dependent on the types of phosphoinositides present, but this requires further investigation. A combinatorial code of phosphoinositides and proteins present in the plasma membrane or in the membrane of intracellular organelles could thus define the protein composition of local microdomains. Given that a phosphoinositide species can be quickly converted into different ones using kinases and phosphatases, such a protein-clustering mechanism allows for very rapid conversion of local microdomains.

EXPERIMENTAL PROCEDURES

Molecular Biology

N-Venus or C-Venus was PCR amplified from TriFC (Rackham and Brown, 2004) using the following primers listed in Table S2: VenusN-F, VenusN-R, VenusC-F, and VenusC-R. PH-GRP_1 was excised using BglII and KpnI from GFP-PH-GRP_1 pUAST (Khuong et al., 2010), and VenusN or VenusC were ligated with GRP_1-PH in the NotI and KpnI sites in pUASTattB (Bischof et al., 2007) and sequenced, and transgenic animals were generated by PhiC31-mediated integration on the third chromosome (UAS-N-Venus in 3L:2376116, VK00031 and UAS-C-Venus in 3R:81372, VK00007; Venken et al., 2006) (GenetiVision).

Lyn11-FRB and FKBP-p85 were PCR amplified (Suh et al., 2006) using Lyn11-F and Lyn11-R; p85-F and p85-R, listed in Table S2, and ligated into the NotI and KpnI sites of pUASTattB and sequenced, and transgenic animals were generated by PhiC31-mediated integration (UAS-Lyn11-FRB in 2L:1584486, VK00037 and UAS-FKBP-p85 in 3L:11062953, attP2; Groth et al., 2004).

The PH-GRP1-mCherry reporter (residues 261–385 of human GRP1 [Swiss-Prot O43739] fused N-terminally to mCherry) used to label PC12 membrane sheets was prepared by expression of a synthetic gene (Genscript) inserted using the NdeI and EcoRI restriction sites into pET-28a(+) in *E. coli* and the protein was purified as described in van den Bogaart et al. (2011). Codon usage was optimized for expression in *E. coli* (K12).

PC12 membrane sheets were generated as described in van den Bogaart et al. (2011).

HA-syntaxin1A^{WT} and HA-syntaxin1A^{KARRAA} were constructed by recombination in pFL44S{w+}-attB in *Saccharomyces* cerevisiae (Merhi et al., 2011) using partially overlapping PCR fragments amplified from BACR15J11 (BACPAC Resources Center [BPRC]) using the primers listed in Table S2. Recombined constructs were sequenced and transgenic animals were generated using PhiC31-mediated integration in 2L: 5108448, attP40 (Groth et al., 2004) (Genetic Services).

Fly Stocks and Temperature Sensitivity

All flies were kept on standard cornmeal and molasses medium and genotypes of animals used are listed in Table S3. For rapamycin feeding, crosses were placed on food mixed with 2 μM rapamycin.

Vials with 10–20 flies were placed in a water bath of the indicated temperatures and time periods. Paralysis of flies was scored as the number of flies that no longer stood up.

GUVs

GUVs were composed of an 8:2 molar ratio of DOPC and DOPS (1,2-dioleoyl-sn-glycero-3-phosphatidylcholine and -serine; Avanti Polar Lipids). The membranes were labeled with 1.5 mol% DiO (3,3′-dioctadecyloxacarbocyanine; Invitrogen). The GUVs were formed by the drying rehydration procedure, as described in van den Bogaart et al. (2011). Briefly, 1 mg/ml total lipid concentration in methanol was mixed with 1.5 mol% dioleoyl-PiP3 (1,2-dioleoyl-sn-glycero-3-[phosphoinositol-3′,4′,5′-trisphosphate]; Avanti Polar Lipids) in a 1:2:0.8 volume mixture of chloroform, methanol, and water. Subsequently, 3 mol% of Atto647N-syntaxin-1A (residues 257-288; Atto647N from Atto-Tec)

in 2,2,2-trifluoroethanol (TFE) was added to the lipid mixture. We then dried 1 μl on a microscope coverslip for 2 min at 50°C–60°C, followed by rehydration in 20 mM HEPES (pH 7.4). GUVs were imaged using a confocal microscope.

FRET Competition Assay

Competitive binding experiments were performed as described in Murray and Tamm (2009) by recording emission spectra of 100-nm-sized liposomes composed of a 4:1 molar ratio of DOPC/DOPS and prepared by extrusion through 100 nm polycarbonate membranes as described in van den Bogaart et al. (2007), with a 1:5,000 molar protein-to-lipid ratio of Atto647N-labeled Syntaxin1A (residues 257–288) and 1:5,000 of bodipy-labeled PI(4,5)P_2 (bodipy-TMR-PI(4,5)P_2,C16; Echelon Biosciences). No additional lipid was added or 1:5,000 or 1:500 of unlabeled PI(4,5)P_2 or 1:5,000 of unlabeled PI(3,4,5)P_2 was added. Excitation was at 544 nm and the excitation and emission slit widths were 1 nm and 5 nm, respectively. A spectrum in the presence of 0.05% Triton X-100 was recorded to correct for the fluorescence crosstalk (gray).

Immunohistochemistry and Superresolution Imaging

Immunohistochemistry was performed as described in Kasprowicz et al. (2008), except for Syntaxin1A labeling; larval fillets were fixed for 15 min in Bouin's fixative and fixed larvae were blocked with 0.25% BSA and 5% NGS in PBS. Antibodies used were the following: Ms anti-FasII^{1D4} 1:20 (Vactor et al., 1993), Ms anti-DLG^{4F3} 1:250 (Parnas et al., 2001), Ms anti-CSP^{6D6} 1:50 (Zinsmaier et al., 1994), Ms anti-BRP^{NC82} 1:100 (Wagh et al., 2006), Ms anti-Syntaxin^{8C3} 1:20 (Schulze and Bellen, 1996) (Developmental Hybridoma Studies Bank), Rb anti-Dap160 1:200 (Roos and Kelly, 1998), Rb anti-Endo 1:200 (Verstreken et al., 2002), anti-HA 1:200, and Rb anti-RBP 1:500 (Liu et al., 2011). GFP or Venus was not visualized with antibodies but their fluorescence was imaged directly. Images were captured on a Zeiss 510 META or Leica DM 6000CS confocal microscope with a 63× NA 1.4 oil lens. Labeling intensity in single section confocal images was quantified as the mean gray value of boutonic fluorescence corrected for background in the muscle; all quantifications were performed on confocal images. Intensity line plots were generated by quantifying boutonic circumference fluorescence intensity in ImageJ and plotting the intensity values versus the normalized bouton circumference. For PiMP, images were captured using a Leica DM 6000CS with 63× NA 1.4 oil lens as described in Munck et al. (2012). Briefly, 200 images of the same field were scanned using low laser power and these bleaching traces were transformed to match 5% bleaching per frame. The deviation of the bleaching per pixel from the average bleaching per frame was determined and the bleach traces were then filtered using a Mexican hat filter. Bleach traces were then summed and corrected for original image linearity as described in Munck et al. (2012). SR-SIM images were acquired on a Zeiss Elyra system using a 63× NA 1.4 oil lens and three rotations. The percent overlap in Syntaxin1A labeling and RBP labeling was quantified by thresholding the boutonic labeling of either marker and calculating the number of pixels positive for both Syntaxin1A and RBP (multiply) divided by the number of Syntaxin1A-positive pixels.

PC12 membrane sheets were fixed in 4% paraformaldehyde in PBS and immunolabeled with Atto647N-NHS-ester (Atto-Tec)-labeled primary antibody anti-Syntaxin1A^{HPC1} (Sigma). Membrane sheets were incubated with 170 nM PH-GRP1 in 3% (w/v) BSA/PBS for 20 min at room temperature. Sheets were washed in PBS and imaged in PBS with TMA-DPH (1-(4-trimethylammoniumphenyl)-6-phenyl-1,3,5-hexatriene; Invitrogen) as described in van den Bogaart et al. (2011). Imaging used the following filters: TMA-DPH: 365/10 | 400LP | 460/50; mCherry: 565/30 | 593 | 645/75; Atto647N: 620/40 | 660LP | 700/75.

Electrophysiology, FM1-43 Imaging, and Electron Microscopy

Two-electrode voltage-clamp experiments were performed using modified HL-3 with 0.5 mM $CaCl_2$ as described in Khuong et al. (2010) and Verstreken et al. (2009). FM1-43 labeling was performed and data quantified as described in Khuong et al. (2010) and Verstreken et al. (2008).

For transmission electron microscopy, third-instar larvae were dissected in modified HL-3 and prepared as described in Uytterhoeven et al. (2011).

Statistical Analysis

Statistical analysis was performed using the appropriate t test or ANOVA model with Tukey's or Dunnett's post hoc tests for pairwise comparisons between groups.

SUPPLEMENTAL INFORMATION

Supplemental Information includes three figures and three tables and can be found with this article online at http://dx.doi.org/10.1016/j.neuron.2013.01.025.

ACKNOWLEDGMENTS

We thank the Bloomington, VDRC, and Harvard *Drosophila* stock centers and the Developmental Studies Hybridoma bank and Bruno André, Hugo Bellen, Chris Brown, Carlos Dotti, Bassem Hassan, Matthew Holt, Elsa Lauwers, and Tobias Meyer for reagents, help, or discussions, as well as members of the Verstreken laboratory for comments. We thank Sebastian Munck from the VIB Bio Imaging Core and LiMoNe facility and KU Leuven cell imaging core facility. Support was provided by a Marie Curie Excellence grant (MEXT-CT-2006-042267), an ERC Starting Grant (260678), FWO grants to P.V., an IUAP by BELSPO, the Research Fund KU Leuven, the Francqui Foundation, the Hercules Foundation, and VIB.

Accepted: January 18, 2013
Published: March 20, 2013

REFERENCES

Aoyagi, K., Sugaya, T., Umeda, M., Yamamoto, S., Terakawa, S., and Takahashi, M. (2005). The activation of exocytotic sites by the formation of phosphatidylinositol 4,5-bisphosphate microdomains at syntaxin clusters. J. Biol. Chem. *280*, 17346–17352.

Arendt, K.L., Royo, M., Fernández-Monreal, M., Knafo, S., Petrok, C.N., Martens, J.R., and Esteban, J.A. (2010). PIP3 controls synaptic function by maintaining AMPA receptor clustering at the postsynaptic membrane. Nat. Neurosci. *13*, 36–44.

Bischof, J., Maeda, R.K., Hediger, M., Karch, F., and Basler, K. (2007). An optimized transgenesis system for Drosophila using germ-line-specific phiC31 integrases. Proc. Natl. Acad. Sci. USA *104*, 3312–3317.

Britton, J.S., Lockwood, W.K., Li, L., Cohen, S.M., and Edgar, B.A. (2002). Drosophila's insulin/PI3-kinase pathway coordinates cellular metabolism with nutritional conditions. Dev. Cell *2*, 239–249.

Christian, D.A., Tian, A., Ellenbroek, W.G., Levental, I., Rajagopal, K., Janmey, P.A., Liu, A.J., Baumgart, T., and Discher, D.E. (2009). Spotted vesicles, striped micelles and Janus assemblies induced by ligand binding. Nat. Mater. *8*, 843–849.

Clark, J., Anderson, K.E., Juvin, V., Smith, T.S., Karpe, F., Wakelam, M.J., Stephens, L.R., and Hawkins, P.T. (2011). Quantification of PtdInsP3 molecular species in cells and tissues by mass spectrometry. Nat. Methods *8*, 267–272.

Cremona, O., Di Paolo, G., Wenk, M.R., Lüthi, A., Kim, W.T., Takei, K., Daniell, L., Nemoto, Y., Shears, S.B., Flavell, R.A., et al. (1999). Essential role of phosphoinositide metabolism in synaptic vesicle recycling. Cell *99*, 179–188.

Denisov, G., Wanaski, S., Luan, P., Glaser, M., and McLaughlin, S. (1998). Binding of basic peptides to membranes produces lateral domains enriched in the acidic lipids phosphatidylserine and phosphatidylinositol 4,5-bisphosphate: an electrostatic model and experimental results. Biophys. J. *74*, 731–744.

Di Paolo, G., and De Camilli, P. (2006). Phosphoinositides in cell regulation and membrane dynamics. Nature *443*, 651–657.

Di Paolo, G., Moskowitz, H.S., Gipson, K., Wenk, M.R., Voronov, S., Obayashi, M., Flavell, R., Fitzsimonds, R.M., Ryan, T.A., and De Camilli, P. (2004). Impaired PtdIns(4,5)P2 synthesis in nerve terminals produces defects in synaptic vesicle trafficking. Nature *431*, 415–422.

Field, S.J., Madson, N., Kerr, M.L., Galbraith, K.A., Kennedy, C.E., Tahiliani, M., Wilkins, A., and Cantley, L.C. (2005). PtdIns(4,5)P2 functions at the cleavage furrow during cytokinesis. Curr. Biol. *15*, 1407–1412.

Gerber, S.H., Rah, J.C., Min, S.W., Liu, X., de Wit, H., Dulubova, I., Meyer, A.C., Rizo, J., Arancillo, M., Hammer, R.E., et al. (2008). Conformational switch of syntaxin-1 controls synaptic vesicle fusion. Science *321*, 1507–1510.

González-Gaitán, M., and Jäckle, H. (1997). Role of Drosophila alpha-adaptin in presynaptic vesicle recycling. Cell *88*, 767–776.

Gray, A., Van Der Kaay, J., and Downes, C.P. (1999). The pleckstrin homology domains of protein kinase B and GRP1 (general receptor for phosphoinositides-1) are sensitive and selective probes for the cellular detection of phosphatidylinositol 3,4-bisphosphate and/or phosphatidylinositol 3,4,5-trisphosphate in vivo. Biochem. J. *344*, 929–936.

Groth, A.C., Fish, M., Nusse, R., and Calos, M.P. (2004). Construction of transgenic Drosophila by using the site-specific integrase from phage phiC31. Genetics *166*, 1775–1782.

Hammond, G.R., Fischer, M.J., Anderson, K.E., Holdich, J., Koteci, A., Balla, T., and Irvine, R.F. (2012). PI4P and PI(4,5)P2 are essential but independent lipid determinants of membrane identity. Science *337*, 727–730.

Heo, W.D., Inoue, T., Park, W.S., Kim, M.L., Park, B.O., Wandless, T.J., and Meyer, T. (2006). PI(3,4,5)P3 and PI(4,5)P2 lipids target proteins with polybasic clusters to the plasma membrane. Science *314*, 1458–1461.

James, D.J., Khodthong, C., Kowalchyk, J.A., and Martin, T.F. (2008). Phosphatidylinositol 4,5-bisphosphate regulates SNARE-dependent membrane fusion. J. Cell Biol. *182*, 355–366.

Kasprowicz, J., Kuenen, S., Miskiewicz, K., Habets, R.L., Smitz, L., and Verstreken, P. (2008). Inactivation of clathrin heavy chain inhibits synaptic recycling but allows bulk membrane uptake. J. Cell Biol. *182*, 1007–1016.

Khuong, T.M., Habets, R.L., Slabbaert, J.R., and Verstreken, P. (2010). WASP is activated by phosphatidylinositol-4,5-bisphosphate to restrict synapse growth in a pathway parallel to bone morphogenetic protein signaling. Proc. Natl. Acad. Sci. USA *107*, 17379–17384.

Kittel, R.J., Wichmann, C., Rasse, T.M., Fouquet, W., Schmidt, M., Schmid, A., Wagh, D.A., Pawlu, C., Kellner, R.R., Willig, K.I., et al. (2006). Bruchpilot promotes active zone assembly, Ca2+ channel clustering, and vesicle release. Science *312*, 1051–1054.

Koh, T.W., Verstreken, P., and Bellen, H.J. (2004). Dap160/intersectin acts as a stabilizing scaffold required for synaptic development and vesicle endocytosis. Neuron *43*, 193–205.

Kooijman, E.E., King, K.E., Gangoda, M., and Gericke, A. (2009). Ionization properties of phosphatidylinositol polyphosphates in mixed model membranes. Biochemistry *48*, 9360–9371.

Kweon, D.H., Kim, C.S., and Shin, Y.K. (2002). The membrane-dipped neuronal SNARE complex: a site-directed spin labeling electron paramagnetic resonance study. Biochemistry *41*, 9264–9268.

Lam, A.D., Tryoen-Toth, P., Tsai, B., Vitale, N., and Stuenkel, E.L. (2008). SNARE-catalyzed fusion events are regulated by Syntaxin1A-lipid interactions. Mol. Biol. Cell *19*, 485–497.

Littleton, J.T., Chapman, E.R., Kreber, R., Garment, M.B., Carlson, S.D., and Ganetzky, B. (1998). Temperature-sensitive paralytic mutations demonstrate that synaptic exocytosis requires SNARE complex assembly and disassembly. Neuron *21*, 401–413.

Liu, K.S., Siebert, M., Mertel, S., Knoche, E., Wegener, S., Wichmann, C., Matkovic, T., Muhammad, K., Depner, H., Mettke, C., et al. (2011). RIM-binding protein, a central part of the active zone, is essential for neurotransmitter release. Science *334*, 1565–1569.

Marie, B., Sweeney, S.T., Poskanzer, K.E., Roos, J., Kelly, R.B., and Davis, G.W. (2004). Dap160/intersectin scaffolds the periactive zone to achieve high-fidelity endocytosis and normal synaptic growth. Neuron *43*, 207–219.

Martin, T.F. (2012). Role of PI(4,5)P(2) in vesicle exocytosis and membrane fusion. Subcell. Biochem. *59*, 111–130.

McLaughlin, S., and Murray, D. (2005). Plasma membrane phosphoinositide organization by protein electrostatics. Nature *438*, 605–611.

Merhi, A., Gérard, N., Lauwers, E., Prévost, M., and André, B. (2011). Systematic mutational analysis of the intracellular regions of yeast Gap1 permease. PLoS ONE *6*, e18457.

Milosevic, I., Sørensen, J.B., Lang, T., Krauss, M., Nagy, G., Haucke, V., Jahn, R., and Neher, E. (2005). Plasmalemmal phosphatidylinositol-4,5-bisphosphate level regulates the releasable vesicle pool size in chromaffin cells. J. Neurosci. *25*, 2557–2565.

Munck, S., Miskiewicz, K., Sannerud, R., Menchon, S.A., Jose, L., Heintzmann, R., Verstreken, P., and Annaert, W. (2012). Sub-diffraction imaging on standard microscopes through photobleaching microscopy with non-linear processing. J. Cell Sci. *125*, 2257–2266.

Murray, D.H., and Tamm, L.K. (2009). Clustering of syntaxin-1A in model membranes is modulated by phosphatidylinositol 4,5-bisphosphate and cholesterol. Biochemistry *48*, 4617–4625.

Oatey, P.B., Venkateswarlu, K., Williams, A.G., Fletcher, L.M., Foulstone, E.J., Cullen, P.J., and Tavaré, J.M. (1999). Confocal imaging of the subcellular distribution of phosphatidylinositol 3,4,5-trisphosphate in insulin- and PDGF-stimulated 3T3-L1 adipocytes. Biochem. J. *344*, 511–518.

Parnas, D., Haghighi, A.P., Fetter, R.D., Kim, S.W., and Goodman, C.S. (2001). Regulation of postsynaptic structure and protein localization by the Rho-type guanine nucleotide exchange factor dPix. Neuron *32*, 415–424.

Rackham, O., and Brown, C.M. (2004). Visualization of RNA-protein interactions in living cells: FMRP and IMP1 interact on mRNAs. EMBO J. *23*, 3346–3355.

Ramaswami, M., Krishnan, K.S., and Kelly, R.B. (1994). Intermediates in synaptic vesicle recycling revealed by optical imaging of Drosophila neuromuscular junctions. Neuron *13*, 363–375.

Raucher, D., Stauffer, T., Chen, W., Shen, K., Guo, S., York, J.D., Sheetz, M.P., and Meyer, T. (2000). Phosphatidylinositol 4,5-bisphosphate functions as a second messenger that regulates cytoskeleton-plasma membrane adhesion. Cell *100*, 221–228.

Roos, J., and Kelly, R.B. (1998). Dap160, a neural-specific Eps15 homology and multiple SH3 domain-containing protein that interacts with Drosophila dynamin. J. Biol. Chem. *273*, 19108–19119.

Schulze, K.L., and Bellen, H.J. (1996). Drosophila syntaxin is required for cell viability and may function in membrane formation and stabilization. Genetics *144*, 1713–1724.

Schulze, K.L., Broadie, K., Perin, M.S., and Bellen, H.J. (1995). Genetic and electrophysiological studies of Drosophila syntaxin-1A demonstrate its role in nonneuronal secretion and neurotransmission. Cell *80*, 311–320.

Slabbaert, J.R., Khuong, T.M., and Verstreken, P. (2012). Phosphoinositides at the neuromuscular junction of Drosophila melanogaster: a genetic approach. Methods Cell Biol. *108*, 227–247.

Spencer, D.M., Wandless, T.J., Schreiber, S.L., and Crabtree, G.R. (1993). Controlling signal transduction with synthetic ligands. Science *262*, 1019–1024.

Suh, B.C., Inoue, T., Meyer, T., and Hille, B. (2006). Rapid chemically induced changes of PtdIns(4,5)P2 gate KCNQ ion channels. Science *314*, 1454–1457.

Sun, Q., Bahri, S., Schmid, A., Chia, W., and Zinn, K. (2000). Receptor tyrosine phosphatases regulate axon guidance across the midline of the Drosophila embryo. Development *127*, 801–812.

Uytterhoeven, V., Kuenen, S., Kasprowicz, J., Miskiewicz, K., and Verstreken, P. (2011). Loss of skywalker reveals synaptic endosomes as sorting stations for synaptic vesicle proteins. Cell *145*, 117–132.

Vactor, D.V., Sink, H., Fambrough, D., Tsoo, R., and Goodman, C.S. (1993). Genes that control neuromuscular specificity in Drosophila. Cell *73*, 1137–1153.

van den Bogaart, G., Mika, J.T., Krasnikov, V., and Poolman, B. (2007). The lipid dependence of melittin action investigated by dual-color fluorescence burst analysis. Biophys. J. *93*, 154–163.

van den Bogaart, G., Meyenberg, K., Risselada, H.J., Amin, H., Willig, K.I., Hubrich, B.E., Dier, M., Hell, S.W., Grubmüller, H., Diederichsen, U., and

Jahn, R. (2011). Membrane protein sequestering by ionic protein-lipid interactions. Nature *479*, 552–555.

Venken, K.J., He, Y., Hoskins, R.A., and Bellen, H.J. (2006). P[acman]: a BAC transgenic platform for targeted insertion of large DNA fragments in D. melanogaster. Science *314*, 1747–1751.

Verstreken, P., Kjaerulff, O., Lloyd, T.E., Atkinson, R., Zhou, Y., Meinertzhagen, I.A., and Bellen, H.J. (2002). Endophilin mutations block clathrin-mediated endocytosis but not neurotransmitter release. Cell *109*, 101–112.

Verstreken, P., Ohyama, T., and Bellen, H.J. (2008). FM 1-43 labeling of synaptic vesicle pools at the Drosophila neuromuscular junction. Methods Mol. Biol. *440*, 349–369.

Verstreken, P., Ohyama, T., Haueter, C., Habets, R.L., Lin, Y.Q., Swan, L.E., Ly, C.V., Venken, K.J., De Camilli, P., and Bellen, H.J. (2009). Tweek, an evolutionarily conserved protein, is required for synaptic vesicle recycling. Neuron *63*, 203–215.

Wagh, D.A., Rasse, T.M., Asan, E., Hofbauer, A., Schwenkert, I., Dürrbeck, H., Buchner, S., Dabauvalle, M.C., Schmidt, M., Qin, G., et al. (2006). Bruchpilot, a protein with homology to ELKS/CAST, is required for structural integrity and function of synaptic active zones in Drosophila. Neuron *49*, 833–844.

Wang, J., Gambhir, A., Hangyás-Mihályné, G., Murray, D., Golebiewska, U., and McLaughlin, S. (2002). Lateral sequestration of phosphatidylinositol 4,5-bisphosphate by the basic effector domain of myristoylated alanine-rich C kinase substrate is due to nonspecific electrostatic interactions. J. Biol. Chem. *277*, 34401–34412.

Wenk, M.R., Pellegrini, L., Klenchin, V.A., Di Paolo, G., Chang, S., Daniell, L., Arioka, M., Martin, T.F., and De Camilli, P. (2001). PIP kinase Igamma is the major PI(4,5)P(2) synthesizing enzyme at the synapse. Neuron *32*, 79–88.

Zinsmaier, K.E., Eberle, K.K., Buchner, E., Walter, N., and Benzer, S. (1994). Paralysis and early death in cysteine string protein mutants of Drosophila. Science *263*, 977–980.

Zoncu, R., Perera, R.M., Sebastian, R., Nakatsu, F., Chen, H., Balla, T., Ayala, G., Toomre, D., and De Camilli, P.V. (2007). Loss of endocytic clathrin-coated pits upon acute depletion of phosphatidylinositol 4,5-bisphosphate. Proc. Natl. Acad. Sci. USA *104*, 3793–3798.